Water Sorption Isotherms and Enthalpies of Water Sorption by Lysozyme using the Quartz Crystal Microbalance/Heat-Conduction Calorimeter

Allan L. Smith†, Hamid M. Shirazi*, and S. Rose Mulligan

Chemistry Department, Drexel University, Philadelphia, PA 19104

† corresponding author; e-mail address, Allan.Smith@Drexel.edu

* Present address: Avecia Ltd, Ink-Jet Ink Division, New Castle, DE, 19720; e-mail address, Hamid.Shirazi@Avecia.Com

Summary

The water sorption isotherm and the water vapor activity dependence of the enthalpy of water sorption $\Delta_{sorp}H^{\circ}$ of lysozyme have been measured at 25˚C. A thin film of lysozyme of mass 250 μg was exposed to H_2O/N_2 mixtures in a quartz crystal microbalance/heat conduction calorimeter (QCM/HCC). The QCM/HCC is a new gravimetric/calorimetric method that measures simultaneously and with high precision the mass change and the corresponding heat flow in a thin film exposed to a gas. $\Delta_{sorp}H^{\circ}$ for lysozyme agrees with previous determinations, although hysteresis effects are evident in the data. No van't Hoff analysis is necessary because sorption enthalpies are measured calorimetrically. The water vapor activity dependence of $\Delta_{sorp}H^{\circ}$ agrees with that measured previously by Bone. As the water content of the lysozyme film drops below10 mass%, $\Delta_{sorp}H^{\circ}$ becomes more exothermic, indicating that water is being bound to the charged or highly polar groups of the solvent-accessible surface of lysozyme. The dynamics of water uptake and release from lysozyme thin films are much slower than in polymer films of comparable thickness. Because the QCM/HCC operates with sub-mg samples, any protein is now amenable to study by this technique.

Keywords

sorption isotherm, water sorption enthalpy, quartz crystal microbalance/heat conduction calorimetry, lysozyme

Introduction

Protein-water interactions are well known to influence both the structure and function of proteins. Gregory [1]is the most recent to have reviewed the hydration of proteins, with previous reviews by Townes [2] , Rupley and Careri [3] , Rupley, Gratton, and Careri [4] and Kuntz and Kauffman [5]. In 1993, Makhatadze and Privalov [6], [7] determined the contribution of hydration to the folding thermodynamics of proteins by using enthalpies, entropies, and heat capacities of transfer of various model compounds from the gas phase into water. A new and improved set of peptide-based group heat capacities for use in protein stability calculations has been presented by Häckel, Hinz, and Hedwig [8] .The relationship between protein hydration and protein structure and function is also important in biotechnological applications of proteins such as enzymes in organic solvents [9], [10], stabilization of liquid protein preparations for pharmaceutical use [11], and food preservation [12]. These reviews describe the many structural, spectroscopic, and thermodynamic methods that have been used over the decades to study biopolymer-water systems.

Studies in this area can be categorized into two groups. Some have employed protein solutions, where the water activity has either been close to unity [6], [7] or it has been controlled by manipulating the percent composition of water-cosolvent mixtures [9]. Others have studied hydrated protein powders, films, or glasses in the presence of water vapor at varying relative humidities. In most cases the intercellular environment in which proteins function *in vivo* resembles hydration states for hydrated powders and films more than dilute solutions [1]. For these low water content states, variation in the amount of internal and surface water for a protein can have pronounced effects on its structure and function. Water vapor sorption isotherms for lyophilized proteins show three regions of the protein where sorbed water may reside [2]:

region(I), binding sites at charged or highly polar groups in the solvent-accessible protein surface (monolayer coverage) . This layer occurs for water content h (g H_2O per g protein) of 0.0 to ~0.1.

region(II), binding sites on the polypeptide backbone and less polar groups (onset of transition from monolayer to multilayer). The water content in region (II) is $0.1 < h < 0.38$.

region(III), condensation of H_2O at very weak binding sites and further growth of water multilayers $(0.38 < h < 1)$.

The few measurements of water sorption enthalpies of proteins show that at high water content the enthalpy of water sorption equals the condensation enthalpy of pure water, -44 kJ mol^{-1}, but increases substantially at lower h as the water molecules bind directly to the protein rather than to each other.

Studying the nature of a protein for a given degree of hydration helps in understanding the chemical stability, conformational stability and activity of the protein. Residual moisture content beyond a monolayer increases the conformational flexibility and the ability of less bound water to mobilize reactants, thereby accelerating decomposition of

the protein. On the other hand, overdrying exposes the surface of the protein and may result in unwanted reactions such as aggregation and ultimately denaturation. The amount of absorbed water also determines the mechanical properties of a protein. Water acts as a plasticizer [1], its addition increasing the free volume and suppressing the glass transition temperature (T_g).

Lüscher-Mattli [13] has reviewed and tabulated certain thermodynamic parameters for biopolymer-water systems. In water sorption experiments, gravimetric measurements of water uptake or release are made on protein samples equilibrated for long periods with different partial pressures of water vapor. By measuring sorption isotherms at different temperatures, isosteric sorption enthalpies of water in proteins have been determined from the van't Hoff equation for ten common proteins, whereas direct calorimetric determinations of water sorption enthalpies have been made for only two proteins, albumen and collagen [13]. Calorimetric studies of water sorption by proteins are thus rare. Yet virtually all proteins function in an aqueous environment, and are profoundly affected by the removal of water.

In this paper, we describe a new method of measuring both the water sorption isotherm and the water sorption enthalpy of a protein as a function of water vapor activity. These measurements are done isothermally on sub-milligram protein samples in the form of a thin film.

Materials and Methods

Many experimental methods in calorimetry and thermal analysis involve measurements of heat and mass changes associated with chemical processes [14], but few, if any, can be applied to studying thermodynamic processes in thin films. A new and highly sensitive gravimetric/calorimetric method which measures simultaneously and with high precision the mass change and the corresponding heat flow in a thin film exposed to a gas has been developed: the quartz crystal microbalance/heat conduction calorimeter, [15] [16]. The basic mass/heat flow sensor [17] is shown in Figure 1.

The mass sensor is a quartz crystal microbalance (QCM), a type of piezoelectric mass-sensing device. The resonant frequency of a quartz plate resonator is inversely proportional to the thickness of the quartz plate. If this thickness is increased by the deposition of material on the surface of the resonator, its frequency will decrease, and this is the basis of the QCM [18]. Sauerbrey [19] showed that the fractional decrease in the fundamental frequency Δf of a QCM upon deposition of a uniform mass per unit area $\Delta m/A$ of material on its surface is given by:

$$\frac{\Delta f}{f_o} = \frac{-\Delta l}{l_o} = \frac{-2 f_o \Delta m}{A\sqrt{\rho\mu}}$$

Here ℓ_0 is the thickness of the quartz plate, $\Delta\ell$ is the change in thickness due to deposition of mass, f_0 is the resonant frequency, Δm is the mass deposited on area A, ρ is the density of quartz and μ is the shear modulus of quartz. For our device (Maxtec, Inc., Santa Fe Springs, CA, part 149211), f_0 = 5 MHz, and the Sauerbrey equation can be expressed as $\delta f = -57\ \delta m/A$, where the frequency shift is in Hz, the mass change in micrograms, and the area in cm^2. Janshoff, Galla, and Steinem [20] have reviewed the widespread use of these devices as biosensors when coated with films that interact with specific biomolecules.

In heat flow calorimetry, the thermal power, or heat flow from sample to surroundings, is measured as a function of time, and the total heat associated with the chemical process is determined by integration over time. Wadsö [21] has reviewed trends in heat conduction calorimetry. The sensor in a heat conduction calorimeter is a thermopile or thermocouple plate (Melcor Inc., Trenton NJ, part FC0.45-66-05). These modules are widely used as thermoelectric heat pumps in computers and other electronics, because when a current passes through the module a temperature difference is generated across its faces. By measuring the voltage generated when heat flows through the faces of the module, the thermoelectric heat pump can be used as a heat flow sensor.

The thermal power P detected by a heat conduction calorimeter is given by the Tian equation [21],

$$P = \frac{dQ}{dt} = \frac{1}{S}\left[U + \tau\left(\frac{dU}{dt}\right)\right]$$

where P is the thermal power, S is the thermopile sensitivity, U is the thermopile voltage, and τ is the time constant of the calorimeter. At steady state, U = S P, and the output voltage is proportional to the thermal power. Since the QCM itself dissipates thermal power when resonating, this power can be used to calibrate the thermopile sensors. By tuning the frequency of a signal generator or impedance analyzer to the QCM resonant frequency and measuring the RMS current and voltage I_{rms} and V_{rms}, and the steady-state heat flow or thermal power P, the thermopile sensitivity can be determined [16].

Both sample and reference combinations of the heat/mass flow sensor are mounted in a constant temperature bath regulated to ±0.0001˚C. The sample QCM is coated with a thin (~ 1.0 μm) film of the protein. By providing both QCM surfaces with the same slow flow of nitrogen/water vapor mixtures at 25˚C and ambient pressure,[16] we have been able to measure simultaneously the change in mass per unit area (to ± 2 ng/cm^2) and the resulting heat flows (to ± 50 nW) when the film on the sample QCM surface takes up or releases the water vapor.

Lysozyme, a globular protein of mass 14.6 kDa, is a mucolytic enzyme with antibiotic properties. Lysozyme has been studied extensively, in particular with respect to its hydration/dehydration behavior at different water contents. Lysozyme from hen egg white was obtained from Sigma (L-6876, Lot 65H7025). The lyophilized protein

contained (approximately) 5% buffer salts (sodium acetate and sodium chloride). The lysozyme was used without further purification to prepare a dilute solution in deionized H_2O.

Piranha solution (one part 30% H_2O_2 in three parts 98% H_2SO_4) was used to clean the QCM gold electrode surfaces before coating them. The QCM was immersed in Piranha solution for 3 minutes and rinsed with deionized water. On the larger top electrode of the QCM a thin film of lysozyme solution was deposited using an air brush (Badger, Franklin Park, IL, Model 200) held about 20 centimeters above the QCM surface. Using research-grade N_2 as the carrier gas a thin film was applied by moving the airbrush at a steady rate parallel to the QCM surface. Two to three short strokes of the solution were applied after which about four/five short strokes of only the nitrogen carrier gas were sprayed across the surface to allow for some drying of the thin film. The process was repeated until a thin film was visibly observable on the QCM surface.

The coated QCM was then fitted with an O-ring and clamped into the sample chamber of the instrument. A 1.98 cm^2 area of the gold electrode surface covered with lysozyme was exposed to the gas flow. The sample and reference chambers were then immersed into the constant temperature bath (Tronac, Provo, UT, Model 1250, 25^{o}C $\pm$0.0001^{o}C). Both the sample and reference QCM surfaces were exposed initially to a flow (40 cc/min total) of the nitrogen carrier gas containing 28,000 PPM of water vapor. The water vapor activity a_{H2O} during each step was calculated as p_{H2O}/p_{H2O}°, the ratio of water vapor pressure to saturation vapor pressure at 25.00˚C. Thus, 28,000 PPM corresponds to $a_{H2O} = 0.895$.

Each experiment began with a six-hour conditioning period starting at the second highest a_{H2O} for that run. It was felt that this conditioning was needed in order to minimize the effect of the prior history of the film sample on the observed mass and heat flow changes when an actual run began. The six-hour period was chosen arbitrarily, and may have to be increased to eliminate hysteresis effects (vide *infra).* The first experiment started with $a_{H2O} = 0.895$, and five subsequent stepwise reductions in a_{H2O} were made after 4000 sec intervals until $a_{H2O} = 0.735$. Mass and thermal power measurements were taken at 2 second intervals over a cycle of five steps of increasing a_{H2O} and five steps of decreasing a_{H2O}, with equilibration periods of 4000 sec at each a_{H2O}. Each successive experiment began at the lowest a_{H2O} from the previous experiment. The six-hour conditioning period was repeated for each experiment. The conditions in the six experiments are summarized in Table I. The mass signals in these runs are shown in Figure 2. The corresponding thermal power signal for the experiment with highest water vapor activity range is shown in Figure 3.

At the end of all experiments, thermal calibration of the thermopile in contact with the lysozyme-coated QCM was performed by measuring I_{rms} and V_{rms} at its resonant frequency, as described previously [16].

Two independent methods were used to calculate the mass of the lysozyme film. After the thermal calibration experiments the thin film was dried by exposing to dry nitrogen for 48 hrs. Using the Sauerbrey equation and the measured frequency difference between

the dry sample and reference QCM, the mass of the lysozyme film was determined to be 250.9$\pm$ 0.1 μg. The film was then dissolved in a known volume of deionized water and its UV absorbance was recorded. An absorbance *vs.* concentration curve was made from UV absorption measurements of four lysozyme aqueous stock solutions, each solution then diluted in half three times. UV measurements led to a calculated mass of the lysozyme film of 245 $\pm$ 7 μg. From the density [22] and the mass of the lysozyme film, the volume was calculated to be 2.00×10^{-4} cm^3. This volume and known area of coverage (1.98 cm^2) yielded a dry film thickness of 1.01 $\pm$ 0.01 μm.

Results

The stepwise thermal changes associated with each hydration/dehydration event are obtained from the integrated thermal power signal, shown in Figure 4. To construct such a plot from the thermal power plot (Figure 3), a baseline needed to be established before integrating the signals. Using Origin (Microcal Software, Inc.), the baseline of a Figure 3 trace was defined with a number of user-defined points between each peak. Estimated precision of a given determination of Q by integration is ± 5%.

Since both mass uptake and dissipated thermal power are simultaneously measured, the heat evolved per mole of sorbed water $Q/n_{H2O} = \int P(t)dt/ n_{H2O}$ can be computed as a function of time. This quantity is plotted in Figure 5 for two experiments, $0.096< a_{H2O}<0.259$ and $0.735< a_{H2O}<0.895$. For a given interval of constant a_{H2O} , baselines are determined by assuming zero mass and thermal power signals at the beginning of the interval. The large transients are due to the 50 sec time constant of the thermopiles, and could be eliminated by employing the Tian equation to give instantaneous P(t) signals if desired. If thermal equilibrium were achieved towards the end of each period of constant a_{H2O}, then Q/n_{H2O} would approximate the partial molar enthalpy of water vapor sorption $\Delta_{sorp}H^\circ$ at that a_{H2O}. Computed Q/n_{H2O} values were averaged for the last 500 sec of each constant activity interval for all the experiments of Table I to determine $\Delta_{sorp}H$ as a function of a_{H2O}. The results are shown in Figure 6.

A water sorption isotherm for a protein is a plot of water content h (g H_2O/g protein) vs. water vapor activity a_{H2O}. Since the total mass of the lysozyme film was measured at the end of the experiments and the mass uptake of water is continuously measured, it is possible to compute water sorption isotherms of lysozyme at 25˚C for each of the experiments listed in Table I. The results are shown in Figure 7. Isotherms for both the hydration (rising steps in a_{H2O}) and dehydration (falling steps in a_{H2O}) periods are given.

Discussion

Figure 6 shows that as the protein film dries out, $\Delta_{sorp}H$ increases. Our interpretation of this trend is that for low a_{H2O} the water is binding to regions I and II of the protein (*vide supra*). The few other measurements of $\Delta_{sorp}H$ in proteins at different hydration levels [13] also show this trend. Figure 6 shows that our data agree with the sorption enthalpy data for lysozyme prior to 1986. Bone [23] has measured sorption isotherms in lysozyme at six temperatures by dielectric loss measurements, and has employed the van't Hoff equation to determine sorption enthalpies as a function of water vapor activity. Our data

are also in agreement with those of Bone. The agreement even extends to the discontinuity in slope of the $\Delta_{sorp}H$ data at 10 mass% H_2O, attributed by Bone to a reordering of the protein-based water. The data of Figure 6 are however more extensive than in previous studies, and are carried out on a much smaller protein sample.

The scatter in the sorption enthalpy data comes from several sources: lack of complete equilibration during constant water vapor activity intervals, and somewhat arbitrary choice of baseline. However, several trends are evident. At high a_{H2O}, the enthalpy of sorption is equal to the enthalpy of condensation of liquid water, -44 kJ mol^{-1} within experimental error (estimated as ± 15% for an individual measurement). Gregory estimates that when proteins are hydrated from the lyophilized dry state, a solution state is achieved at $0.38 < h < 1.0$ protein per g water ($a_{H2O} > 0.99$). Figure 7 shows that the maximum value of h reached in these experiments is 0.22, and yet at this value the water sorption enthalpy is indistinguishable from that of pure water or the dilute protein solution state.

The D'Arcy-Watt model [24] for water sorption has been widely applied to water sorption by proteins. It is comprised of three component isotherms arising from separate processes: (a) monolayer adsorption by strongly binding sites; (b) monolayer adsorption by weakly binding sites, and (c) formation of a multilayer the extent of which is limited by the properties of the substrate. The defining equation is

$$h = \frac{h_p' K_2 a_{H_2O}}{1 + K_2 a_{H_2O}} + K_3 a_{H_2O} + \frac{K_4 K_5 a_{H_2O}}{1 - K_5 a_{H_2O}}$$

where h is the water content of the protein, a_{H2O} is the water vapor activity, K_2 is an equilibrium constant for binding water to the charged or highly polar groups on the solvent-accessible surface, K_3 is an equilibrium constant for binding water to the polypeptide backbone and the less polar sites, K_5 is the equilibrium constant for binding water to the outer multilayers and the bulk, and h_p' and K_4 are additional constants. Table II gives the constants determined when the data of Lüscher-Mattli are fit to the D'Arcy-Watt equation, and Figure 7 shows the contribution of each term to the sorption isotherm.

Our data are in good agreement with these previous measurements except for the curious steps at a_{H2O} values of 0.08, 0.27, 0.41, 0.59, and 0.74. These values correspond to the beginning and end of each of the long experiments shown in Figure 2 and Table I. These experiments involve small stepwise changes of a_{H2O} (~0.031) separated by equilibration times of ~4000 sec. As can be seen from the Figures 2 and 4, the mass and thermal changes during the hydration/dehydration events appear to be leveling off but do not fully reach a flat baseline. Furthermore, hysteresis was observed in both mass uptake and thermal power time series, in that the mass uptake at the end of a given a_{H2O} value in sorption differs from its value in desorption. It is important to realize that prior to the beginning of each such experiment, a_{H2O} was held constant at the highest value in the

subsequent run for six hours. The water content at the beginning of an experiment (lowest a_{H2O}) is thus higher than the sorption isotherm trendline because during the sample preconditioning time the average a_{H2O} was substantially higher. However, despite the hysteresis evident in the mass traces in Figure 2, Figure 7 shows that the (h, a_{H2O}) points for increasing a_{H2O} are in good agreement with those for decreasing a_{H2O} in a given experiment. This behavior, repeated in each run, points to a wide range of dynamical processes in protein hydration and dehydration, one of which is remarkably slow (a characteristic time of many hours) and prevents the achievement of true thermodynamic equilibrium. Gregory [1] indicates that hysteresis in the sorption/desorption isotherm of globular proteins is quite common, and that equilibration times of 1-2 days at a constant water vapor pressure are often needed to assure equilibrium.

As described above, buffer salts were not removed from the lysozyme sample before preparing the film. To account for the possible error in reporting values of lysozyme water sorption in a film containing buffer salts, the accessible surface area of the lysozyme was compared with the available surface area of the ions from the buffer salts. The accessible surface area (ASA) of hen egg white (HEW) lysozyme has been calculated as 6710 Ü^2 [25]. Our total film mass was 250 µg. The protein accounted for 95% of this mass or 238 µg while the buffer salts accounted for 5% or 12 µg. Using the molecular weight of lysozyme (14.6 kDa) and the mass, led to a calculation of 1.6 x 10^{-6} moles of lysozyme or 9.6 x 10^{15} molecules of the protein. Each molecule having the above-mentioned ASA, led to a total lysozyme ASA of 6.4 x 10^{19} Ü^2.

Similarly, using the molecular weight and mass of the buffer salt components (NaCl and NaAc) the number of molecules were calculated. For the ions in the buffer salts, the surface area of a sphere was calculated using the Pauling radius values [26]: 1.8 Ü for O^-, 0.95 Ü for Na^+, and 1.8 Ü for Cl^-. The calculated surface areas were 38.9 Ü^2, 11.3 Ü^2, and 41.2 Ü^2 respectively. These surface area values were then multiplied by the number of ions present as determined from the number of molecules. The total ionic surface area from the buffer salts amounted to 5.3 x 10^{18} Ü^2. This area represents only 8% of the total lysozyme accessible surface area available for the sorption of water molecules. Although hydration energies for ions are likely to be larger than for the non-polar groups on the protein surface, we estimate that the error introduced by ignoring the contribution of the buffer salts is at most 15%. Of course, in the future it would be preferable to remove or at least minimize buffer salts before forming the film.

Lysozyme is one of the few proteins whose crystal structure remains intact at low water vapor activities, enabling single-crystal x-ray studies to determine the subtle changes in secondary structure upon dehydration [27]. The denaturation temperature of lysozyme is 342K for dilute solutions and increases as the protein dehydrates [1]. Fujida and Noda [28] have shown that as the water content of lysozyme decreases from 0.2 h to zero the denaturation temperature increases from 350K to over 400K and the denaturation enthalpy decreases from 200 kJ mol^{-1} to less than 100 kJ mol^{-1}. Gregory has summarized the arguments for the existence of a low temperature glass transition in lysozyme which increases with decreasing water content until at h = 0.10 $T_g \approx 25$ ˚C. This implies that

the slow secondary structural changes in lysozyme that take hours to occur as water is removed are not denaturation yet still contribute to the overall energetics of lysozyme-water interaction.

As Mayer and colleagues have shown [29], a slow unfreezing of segmental motions in lysozyme caused by the binding of water to the protein occurs over a temperature range of 150 K up to the denaturation temperature of 350 K. In these experiments a protein is annealed or physically aged by holding it at a constant temperature T' for up to 60 minutes and then a differential scanning calorimeter (DSC) run is begun. The resulting C_p *vs* T curve exhibits a broad endothermic peak above T' characteristic of a weak glass transition temperature. The sorption of water by dehydrated lysozyme causes an increase in the effective heat capacity C_p. All modes with molecular relaxation times comparable to the annealing period become kinetically unfrozen and tend to achieve their respective energy minima.

In our experiments, increasing the water vapor activity at constant temperature (25˚C) also causes increased segmental motion in lysozyme as the protein approaches a more water-rich environment. The enthalpy of the protein itself must thus increase even at constant T. A molecular model explaining the measured protein hydration enthalpies reported in this work must include both the change in water-protein binding energetics and the change in segmental motion upon hydration or dehydration.

Detailed analysis of the kinetics of approach to a new equilibrium state after a change in relative humidity will be presented in another paper. The mass and thermal signals of Figures 2 and 3 indicate slow dynamical changes in thin lysozyme films exposed to changing relative humidity. Preliminary estimates of a characteristic equilibration time τ were made by assuming a time dependence for the mass signal of the form $m(t) = A + B(t-t_0) + C(1-\exp(-(t-t_0)/\tau)$, where t_0 is the time at which a change in relative humidity is made. The second term was needed in order to account for the observed non-zero slope of the baseline and the presence of hysteresis. Non-linear least-squares analysis of mass traces using this equation gave equilibration times of from 75 to 430 sec. These times are much longer than equilibration times we observed for water absorbed in an aliphatic polyurethane film of comparable molar mass to lysozyme. The data show, remarkably, that at very low a_{H2O} the rate of water uptake and loss by the film is actually faster than at higher a_{H2O}. We interpret these results as showing that there are very slow structural relaxation processes occurring in drying lysozyme films, similar to the slow molecular processes responsible both for the hysteresis observed in most sorption isotherms measured by other techniques.

Quartz crystal microbalance/heat conduction calorimetry is a new experimental method combining isothermal calorimetry and gravimetry, permitting continuous, high sensitivity mass (±2 ng) and heat flow (± 0.05 μW) measurements during gas-solid equilibration. It is not a new method in thermal analysis, which has been defined as "the analysis of a change in sample property which is related to an imposed temperature alteration" [14]. Both sorption isotherms and sorption enthalpies are directly measured, and the dynamics of gas-solid equilibration can also be followed. This experimental method has also been

used [30] to characterize polymer/solvent thermodynamics in thin polyurethane films, the dissolution of hydrogen in palladium and its subsequent use as a hydrogenation catalyst, and the thermodynamics of the formation of single alkylthiol monolayers. Measurements have been made in our laboratory of the effect of moisture on pharmaceutical thin coating materials (K.Thompson and A. L. Smith, in preparation).

The physics of the electroacoustic response of film-coated quartz piezoelectric resonators such as those used in the QCM/HCC is now well understood [18], [31], [32]. The complex impedance of the coated resonator is affected by four film parameters: thickness L , density ρ, shear modulus G', and viscoelastic loss modulus G", with the last two parameters determined at the resonant frequency of the resonator. For acoustically thin films [32] the Sauerbrey equation accurately describes the relationship between change in mass per unit area (the product ρL) and change in resonant frequency, and changes in the mechanical properties of the film (G' and G") do not affect ability of the QCM to measure mass changes. However, for thicker films the (complex) change in impedance of the resonator depends on both the shear and loss modulus of the film. These changes can be measured by using impedance analysis [33]. We are performing such analyses on both protein and polymer films. Initial results show that as thin polymer films absorb solvents such as water they increase the equivalent circuit resistance R of the coated crystal, which in turn implies changes in G' and/or G". Such measurements, done in conjunction with the sorption energetics in the QCM/HCC, should provide valuable insights into the change of protein flexibility with hydration level.

In the experiments described in this paper, both the water content and the water sorption enthalpy of a sub-milligram thin-film sample of lysozyme have been determined as a function of water vapor activity. Results are in agreement with previous studies of lysozyme but the sorption enthalpy data are much more extensive. Determining sorption enthalpies from van't Hoff analysis of sorption isotherms is time consuming and requires large sample sizes. With the present method, no van't Hoff analysis is necessary because sorption enthalpies are measured directly. It is now possible to examine in detail the increase in sorption enthalpy as the water content of the protein approaches a monolayer coverage of the solvent-accessible surface and thus binds to the charged and highly polar groups on the protein. The slow dynamics of protein-water equilibration after step-changes in water vapor activity can now be followed by combined gravimetry/calorimetry at constant temperature, and in lysozyme these studies reveal very slow equilibration kinetics.

Because of the high precision and small sample size of quartz crystal microbalance/heat conduction calorimetry, any protein is now amenable to study, not just classical, well-characterized globular proteins available in large quantities. Such studies could include the hydration equilibria and slow dehydration dynamics of oligopeptides or small proteins exhibiting specific secondary structures such as the α helix or the β sheet, or the effect of single mutations on the hydration energetics.

Figure Captions

Figure 1. The mass/heat flow sensor used in the QCM/HCC

Figure 2. Sorption of water vapor by lysozyme film, mass traces. Water vapor activity changed in a stepwise fashion (see text).
a) $0.735 < a_{H2O} < 0.895$
b) $0.576 < a_{H2O} < 0.735$
c) $0.416 < a_{H2O} < 0.576$
d) $0.259 < a_{H2O} < 0.416$
e) $0.096 < a_{H2O} < 0.259$
f) $0.0 < a_{H2O} < 0.096$

Figure 3. Sorption of water vapor by lysozyme film, thermal power trace, $0.735 < a_{H2O} < 0.895$
(a) thermal power measurements with baseline evaluated using Origin software. 50 points chosen to define baseline.
(b) variable baseline subtracted from trace in part (a)

Figure 4. Integrated thermal power signal for water vapor sorption by lysozyme, $0.735 < a_{H2O} < 0.895$

Figure 5. Heat evolved per mole of water vapor sorbed by lysozyme.
a) $0.735 < a_{H2O} < 0.895$
b) $0.096 < a_{H2O} < 0.259$

Figure 6. Hydration enthalpy of lysozyme as the function of water content in mass %.
(a) QCM/HCC measurements
(b) from temperature dependence of gravimetric measurements by Bone (1996) and Lüscher-Mattli (1986)

Figure 7. The water vapor sorption isotherm for lysozyme.
Curves 1 through 4 are from D'Arcy and Watt (1970):
(1) first term of D'Arcy Watt equation, water sorption in region(I)
(2) second term, weak nonpolar sorption sites, region (II)
(3) sorption at multilayer binding sites, region (III)
(4) combined terms
(5) measurements by QCM/HCC, this work

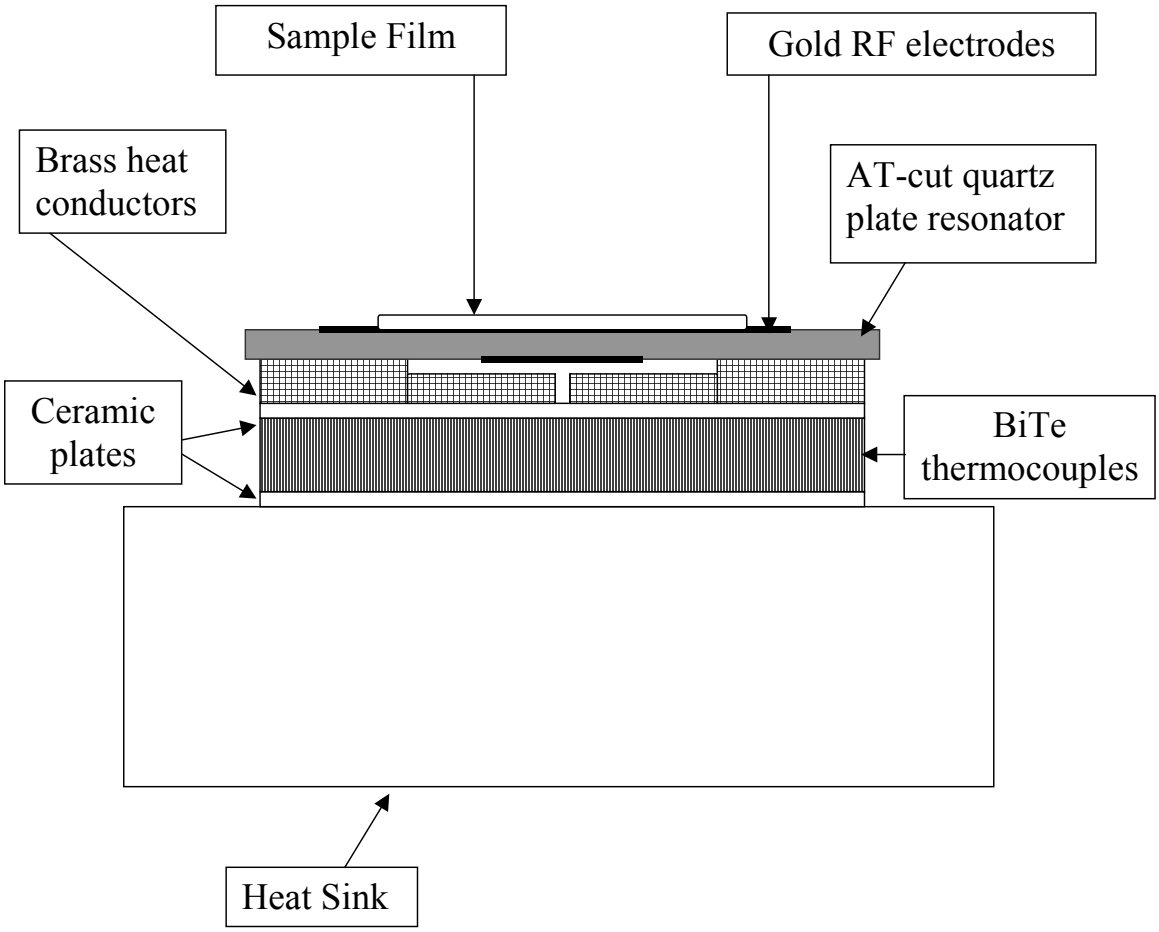
Sample Film
Gold RF electrodes
Brass heat conductors
AT-cut quartz plate resonator
Ceramic plates
BiTe thermocouples
Heat Sink

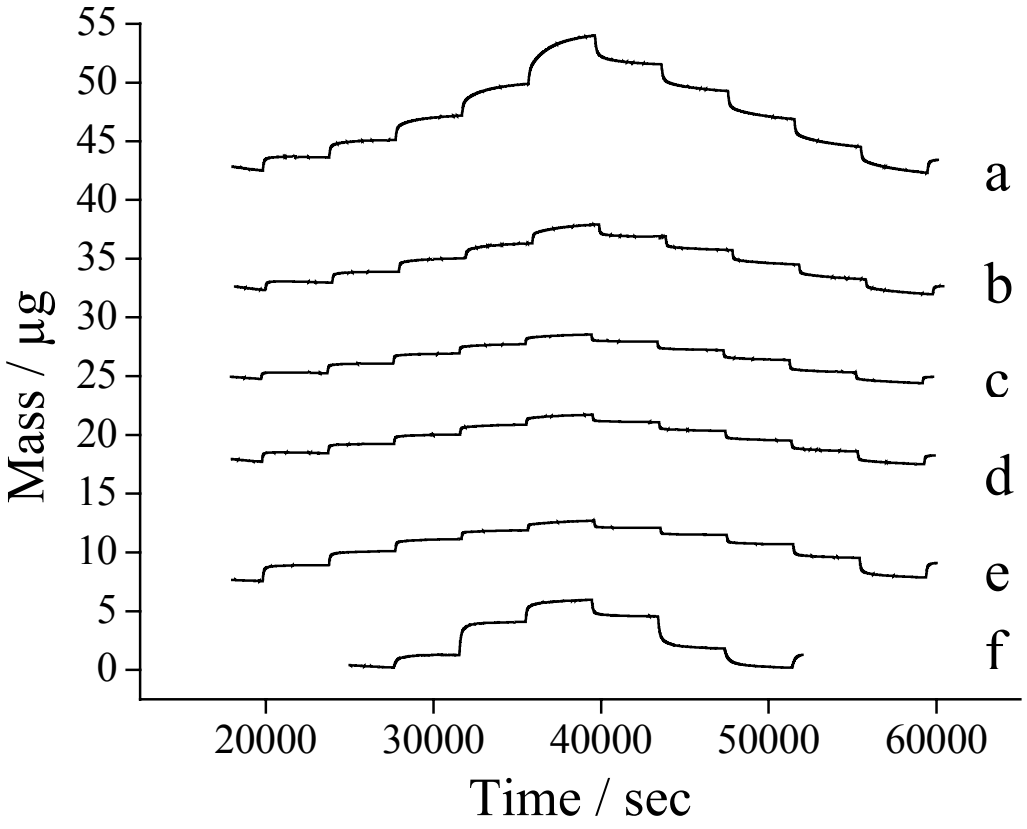
Mass / µg
55
50
45
40
35
30
25
20
15
10
5
0
20000
30000
40000
50000
60000
Time / sec
a
b
c
d
e
f

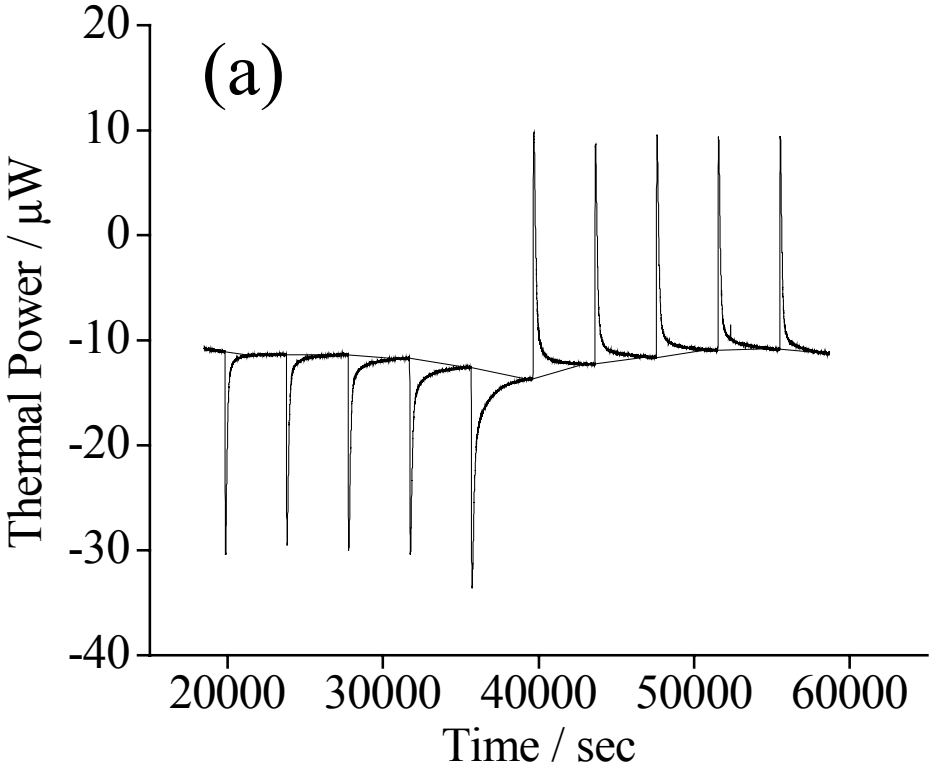
(a)
Thermal Power / µW
20
10
0
-10
-20
-30
-40
20000
30000
40000
50000
60000
Time / sec

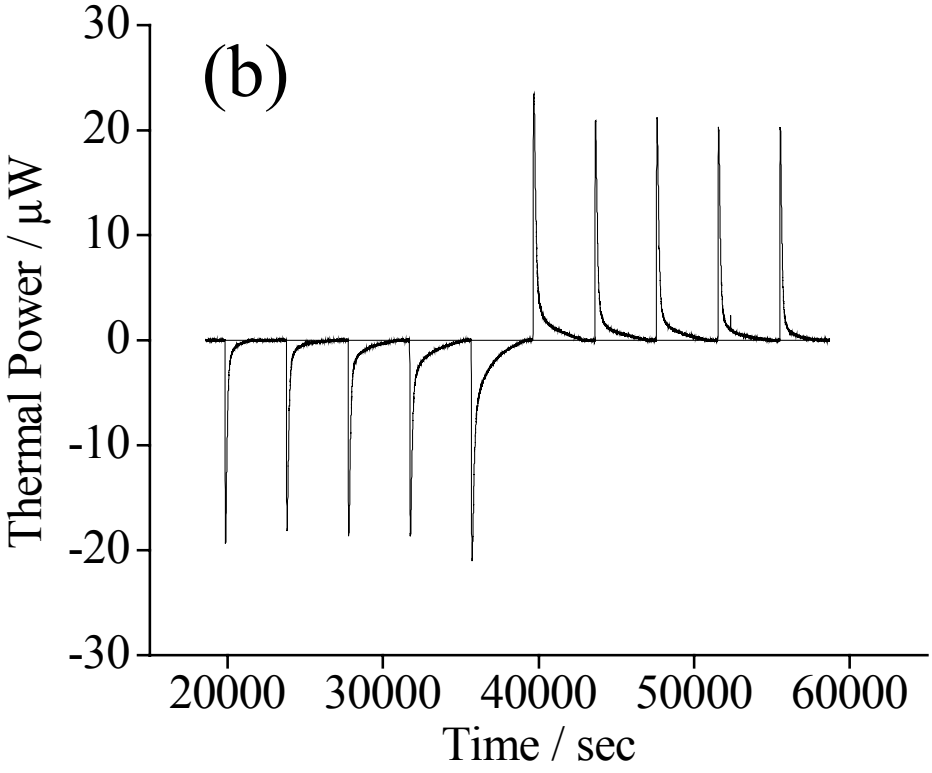
(b)
Thermal Power / µW
30
20
10
0
-10
-20
-30
20000
30000
40000
50000
60000
Time / sec

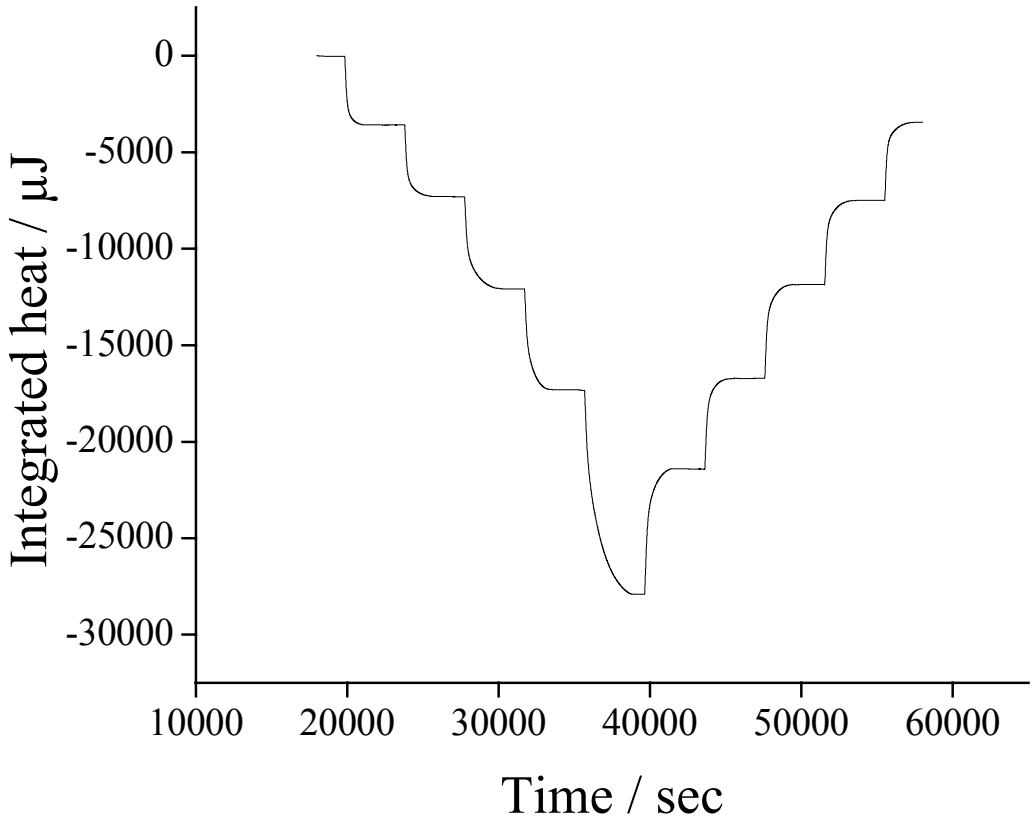
0
-5000
-10000
-15000
-20000
-25000
-30000
Integrated heat / µJ
10000
20000
30000
40000
50000
60000
Time / sec

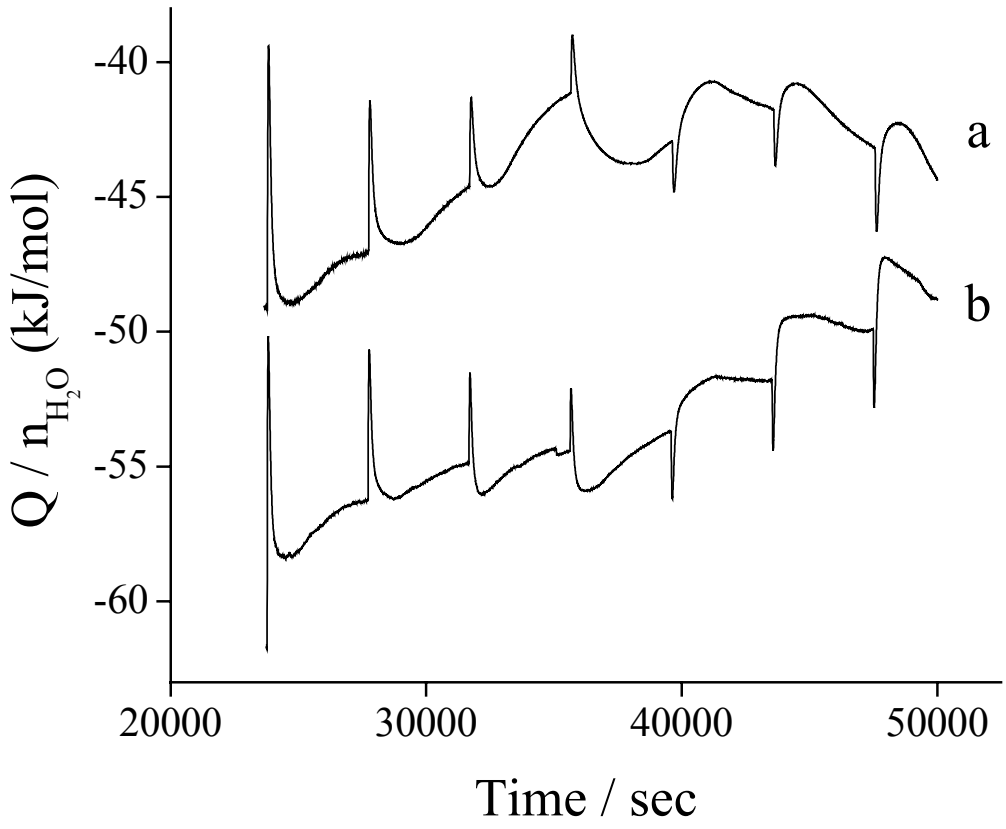
-40
-45
-50
-55
-60
Q / n$_{H_2O}$ (kJ/mol)
a
b
20000
30000
40000
50000
Time / sec

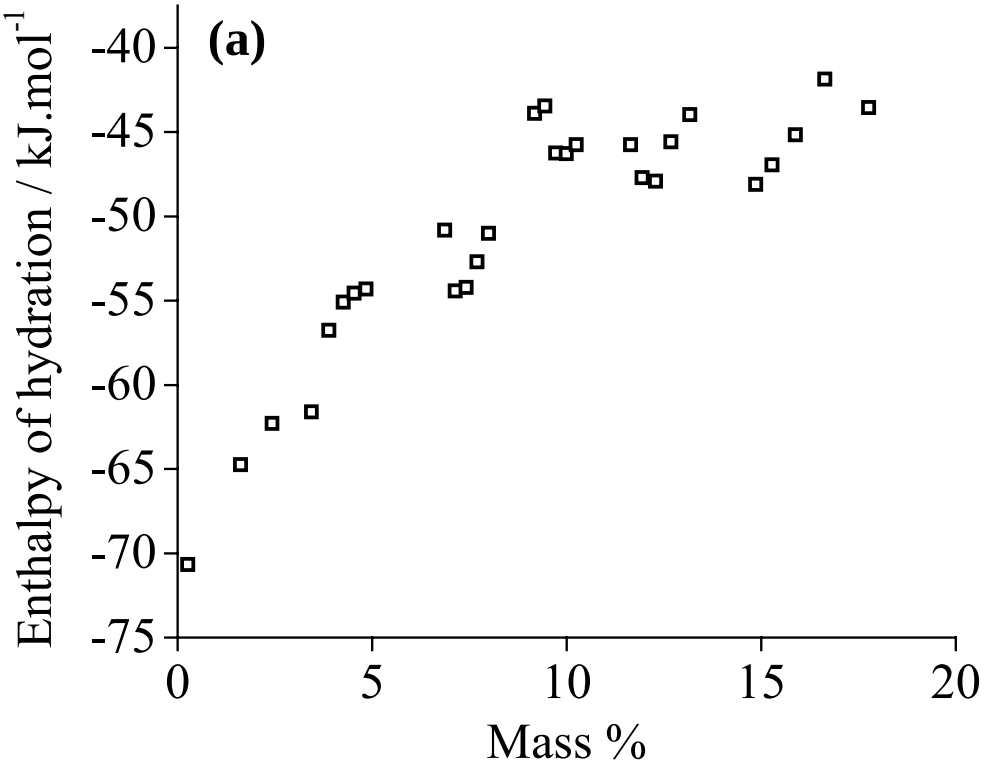
(a)
Enthalpy of hydration / kJ.mol-1
-40
-45
-50
-55
-60
-65
-70
-75
0
5
10
15
20
Mass %

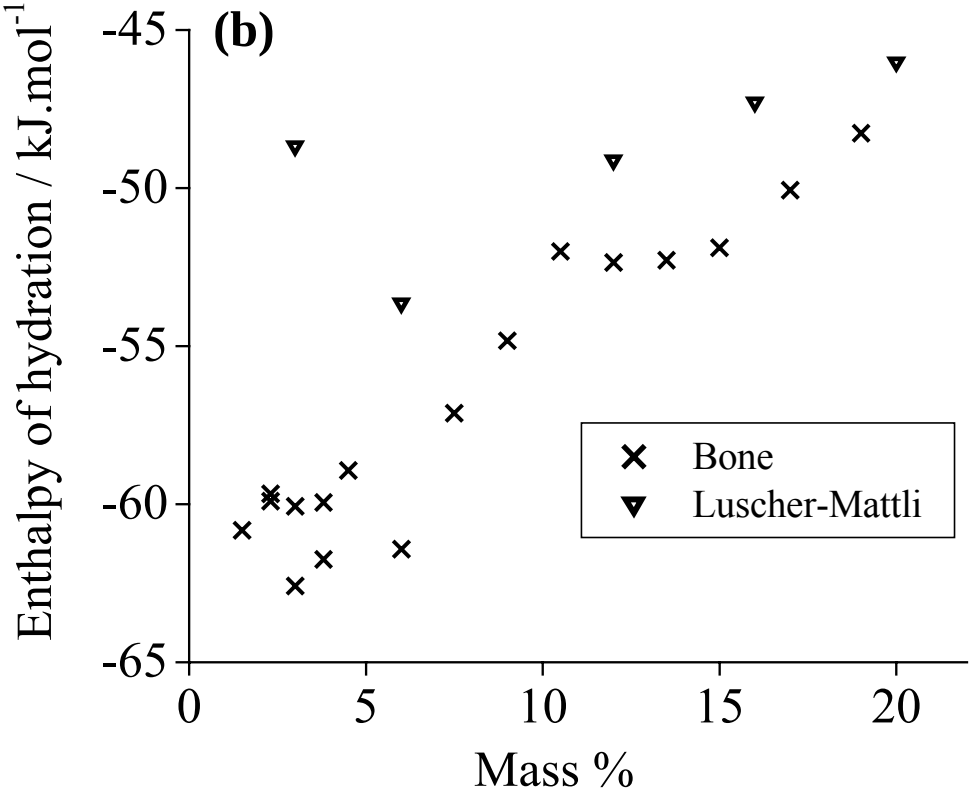
(b)
Enthalpy of hydration / kJ.mol-1
-45
-50
-55
-60
-65
0
5
10
15
20
Mass %
Bone
Luscher-Mattli

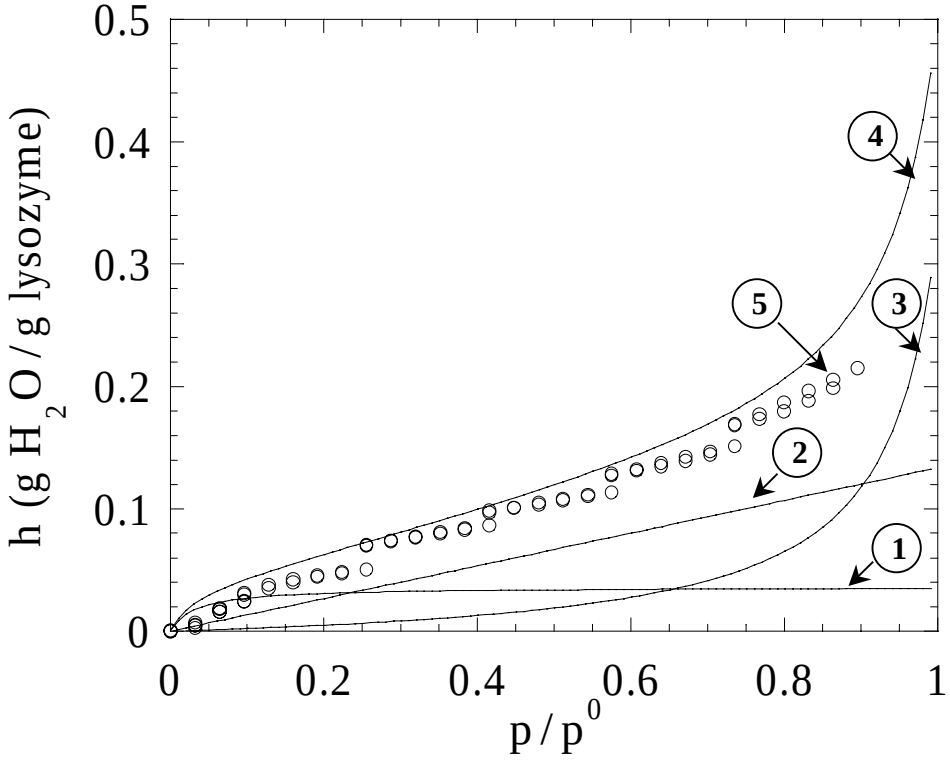
0.5
0.4
0.3
0.2
0.1
0
0
0.2
0.4
0.6
0.8
1
h (g H2O / g lysozyme)
p / p0
1
2
3
4
5

Table I Stepwise changes in water vapor activity during QCM/HCC runs shown in Figure 2. Intervals between stepwise changes are 4000 sec.

experiment	start ppm	end ppm	start a_{H2O}	end a_{H2O}
f	0	1000	0.000	0.032
	1000	2000	0.032	0.064
	2000	3000	0.064	0.096
e	3000	4000	0.096	0.128
	4000	5000	0.128	0.160
	5000	6000	0.160	0.192
	6000	7000	0.192	0.224
	7000	8000	0.224	0.288
d	8000	9000	0.256	0.288
	9000	10000	0.288	0.320
	10000	11000	0.320	0.352
	11000	12000	0.352	0.384
	12000	13000	0.384	0.416
c	13000	14000	0.416	0.448
	14000	15000	0.448	0.480
	15000	16000	0.480	0.512
	16000	17000	0.512	0.544
	17000	18000	0.544	0.576
b	18000	19000	0.576	0.608
	19000	20000	0.608	0.640
	20000	21000	0.640	0.671
	21000	22000	0.671	0.703
	22000	23000	0.703	0.735
a	23000	24000	0.735	0.767
	24000	25000	0.767	0.799
	25000	26000	0.799	0.831
	26000	27000	0.831	0.863
	27000	28000	0.863	0.895

Table II Constants in the D'Arcy-Watt equation for water sorption. Values for the constants are from Luscher-Mattli data fit to the D'Arcy –Watt equation.

Parameter	Value
h'_p	0.0360
K_2	30.9100
K_3	0.1336
K_4	0.0215
K_5	0.9392

References

1 Gregory, R.B. (1995) in Protein-Solvent Interactions (Gregory, R.B., ed.), pp. 191-264, Marcel Dekker, New York.
2 Townes, J.K. (1995) J. Chromatography A 705, 115-127.
3 Rupley, J.A. and Careri, G. (1991) Advances in Protein Chemistry 41, 37-172.
4 Rupley, J.A., Gratton, E. and Careri, G. (1983) in TIBS, Vol. January, pp. 18-22.
5 Kuntz, I.D. and Kauzmann, W. (1974) Advances in Protein Chemistry 28, 239-345.
6 Makhatadze, G.I. and Privalov, P.L. (1993) J. Mol. Biol. 232, 639-659.
7 Privalov, P.L. and Makhatadze, G.I. (1993) J. Mol. Biol. 232, 660-679.
8 Häckel, M., Hinz, H.-J. and Hedwig, G.R. (1999) Journal of Molecular Biology 291, 197-213.
9 Wescott, C.R. and Klibanov, A.M. (1994) Biochimica Et Biophysica Acta-Protein Structure and Molecular Enzymology 1206, 1-9.
10 Klibanov, A.M. (2001) Nature 409, 241-246.
11 Wang, W. (1999) Int. J. of Pharmaceutics 185, 129-188.
12 Slade, L., Levine, H. and Finley, J.W. (1989) Food Sci. and Technol. 29 (Protein Qual. Eff. Process.), 9-124.
13 Luscher-Mattli, M. (1986) in Thermodynamic Data for Biochemistry and Biotechnology (Hinz, H.-J., ed.), pp. 276-296, Springer-Verlag, Berlin.
14 Gallagher, P.K. (1998) Handbook of Thermal Analysis and Calorimetry, Vol. 1, Elsevier, Amsterdam, New York.
15 Smith, A.L., Shirazi, H. and Wadso, I. (1998) in Recent Advances in the Chemistry and Physics of Fullerenes and Related Materials, Vol. 98-8, pp. 576-585, Electrochem. Soc., San Diego, CA.
16 Smith, A.L. and Shirazi, H.M. (2000) J. of Thermal Analysis and Calorimetry 59, 171-186.
17 Smith, A.L. (2000) in U. S. Patent Office 6,106,149,, Allan L. Smith, U. S. A.
18 Buttry, D.A. and Ward, M.D. (1992) Chemical Reviews 92, 1355-1379.
19 Sauerbrey, G. (1959) Z. Physik 155, 206-222.
20 Janshoff, A., Galla, H.-J. and Steinem, C. (2000) Angew. Chem. Int. Ed. 39, 4004-4032.
21 Wadsö, I. (1997) Chem. Soc. Rev. 1997, 79.
22 Durchschlag, H. (1986) in Thermodynamic Data for Biochemistry and Biotechnology (Hinz, H.-J., ed.), pp. 82-83, Spring-Verlag, Berlin.
23 Bone, S. (1996) Phys. Med. Biol. 41, 1265-1275.
24 D'Arcy, R.L. and Watt, I.C. (1970) Trans. Far. Soc. 66, 11236-1245.
25 Lee, B. and Richards, F.M. (1971) Journal of Molecular Biology 55, 379-400.
26 Huheey, J.E., Keiter, E.A. and Keiter, R.L. (1993) Inorganic Chemistry : Principles of Structure and Reactivity, 4th edition ed., HarperCollins, New York.
27 Nagendra, H.G., Sukumar, N. and Vijayan, M. (1998) Proteins-Structure Function and Genetics 32, 229-240.
28 Fujita, Y. and Noda, Y. (1978) Bull. Chem. Soc. Japan 51, 1567-1568.
29 Sartor, G., Mayer, E. and Johari, G.P. (1994) Biophys. J. 66, 249-258.
30 Shirazi, H.M. (2000) in Chemistry,, pp. 336, Drexel University, Philadelphia, PA.
31 Martin, S.J., Bandey, H.L., Cernosek, R.W., Hillman, A.R. and Brown, M.J. (2000) Anal. Chem. 72, 141-149.

32 Hillman, A.R. (2001) Anal. Chem. 73, 540-549.
33 Noel, M.A.M. and Topart, P.A. (1994) Anal. Chem. 66, 484-491.